Development of a Wireless Sensor Network System as basis for Early Warning in Slope Monitoring of the Corinth Canal

G. Hloupis
Department of Electronics, Technological Institute of Athens, Greece

C. Leoussis
Faculty of Geology & Geoenvironment, Department of Geography & Climatology
National & Kapodistrian University of Athens, Greece

V. Pagounis
Department of Surveying Engineering, Technological Institute of Athens, Greece

M. Tsakiri
School of Rural and Surveying Engineering, National Technical University of Athens, Greece

E. Vassilakis
Faculty of Geology & Geoenvironment, Department of Geography & Climatology
National & Kapodistrian University of Athens, Greece

V. Zacharis,
School of Rural and Surveying Engineering, National Technical University of Athens, Greece

Abstract. Corinth Canal is an important technical construction with a significant role in marine and land transportation for Greece. Whilst the main highway of the Corinth bridge is well monitored there is no similar monitoring scheme for landslide failures of the canal walls. This work presents an in-house developed real-time early warning landslide triggering system using wireless sensor network (WSN) nodes. Specifically, for the detection of different types of landslide processes (drift, slide and fall) a set of corresponding MEMS (Micro-Electro-Mechanical Systems) sensors (accelerometer, inclinometer, magnetometer) will be used. These sensors along with radio transmission unit and microprocessor comprise a WSN node. The option for in-situ processing (i.e transmitting only alerts) is possible in order to decrease the communication costs. In conjunction with the proposed WSN system, high accuracy geodetic techniques are used with terrestrial laser scanning (TLS) measurements. TLS is augmenting the point-based system to a spatial -based monitoring system. The paper describes the use of WSN node as triggering device in order to alert the users to begin TLS measurements. A description of the network topology is given along with the implementation of the system in selected control points on the canal walls. Real results are shown and the performance of the system is discussed.

1 Introduction

Structural Health Monitoring (SHM) is a specific field in the context of civil engineering that deals with such issues as damage detection, stability and integrity monitoring of mainly civil infrastructures (e.g. bridges or public buildings) as they represent critical systems requiring constant and careful monitoring. The two major factors in SHM are time-scale of change (i.e. how quickly the change occurs) and severity of change (i.e. degree of change). Examples of the time scale include disaster response (earthquake, explosion, etc.) and continuous health monitoring (ambient vibrations, wind, etc.). The assessment of the integrity of structures is typically carried out manually by experts with specific domain knowledge. This is performed by measurements obtained by specialised instrumentation. However, such practises may easily lead to high costs, insufficient monitoring frequency, or mere mistakes during data collection.

For over a decade, rapid advances in sensors, wireless communication, Micro Electro Mechanical Systems (MEMS), and information technologies have a significantly impact in the improvement of SHM. This is achieved with the use of a monitoring framework based on Wireless Sensor Networks (WSNs) (e.g. Burrati et al., 2009; Culler et al., 2004). Such networks are typically made of a potentially large number of autonomous units, equipped with different sensors in order to measure the required physical quantities; moreover, ad-hoc sensors may be devised for specialized tasks. While the primary purpose of a sensor node is data sensing and gathering toward a base station, through wireless communications, each of them also has limited processing capabilities that may be exploited in order to carry on preliminary operations on raw data. WSNs have already been extensively used for SHM research projects; for example Kim (2004) describes a project aimed at monitoring ambient vibration at the Golden Gate Bridge in San Francisco, Paek et al. (2005) describe the use of WSNs on the monitoring of a seismic test structure and a four-storey office building, Anastasi et al. (2009) discuss the use of WSNs on monitoring critical structures in Sicily, Italy.

Whilst wireless sensors are one of the technologies that can quickly respond to rapid changes of data and send the sensed data to the receiver section in areas where cabling is not available, it has its own limitations such as relatively low amounts of battery power and low memory availability compared to many existing technologies. It does, though, have the advantage of deploying sensors in hostile environments with a minimum of maintenance. This paper describes an approach exploiting the technology of WSNs on the monitoring of the Corinth Canal in Greece. The aim is to develop a low-cost early warning system that in case of warning a geodetic monitoring scheme takes place using   totals station surveying and terrestrial laser scanning (TLS) techniques. The paper describes the proposed early warning triggering system and gives details on the hardware and software component along with the implementation of the system in selected control points on the Canal walls. The paper is structured in 5 sections. Section 2 gives a brief description of the geological characteristics of the Corinth Canal while section 3 describes the design and implementation of the proposed WSN node. Section 4 describes the data processing and gives examples of the results and finally, section 5 gives the concluding remarks for this work.

2 Geological Characteristics of the Corinth Canal

The Corinth Canal (Fig. 1) crosses the Isthmus of Corinth and is of great importance for Mediterranean navigation as well as the railroad and highway connections between southern and central Greece. It is 6.3 km long with a maximum height of 75m above sea level and 10m below sea level. The artificial slopes have an average inclination of 4.5 to 1 (about 75 degrees) and show only minor falls, wedge-type failures and deformations, which developed mostly after severe earthquakes.

Fig. 1 View of the Corinth Canal.

The Canal area has been constructed through a nicely bedded sequence of Pleistocene fluviatile and marine sandstones, conglomerates and recent superficial alluvial deposits (mixtures of clays, sands and gravels), representing a continuous change of the paleo-environmental regime for the last 300 thousand years (Collier and Thompson, 1991). These gently NW dipping, sedimentary discontinuities are frequently crosscut by almost vertical joints and 20-50 fault surfaces, most of them inactive but still decreasing the overall geotechnical properties of the canal artificial slopes (Anagnostopoulos et al., 1991). According to Collier et al. (1992) the Isthmus of Corinth is currently undergoing an uplift phase.

Since the opening of the Canal in 1893 several problems due to local slope instabilities have been reported and at second half of the 20th century 16 local slope instabilities have been occurred in this area (Gkika et al., 2005). The observed instabilities are localized at sites where the horizontal and vertical discontinuities are interwoven with each other and produce wedge type rock falls (Marinos and Tsiambaos, 2008). The only active fault, which

clearly influences the topography, crosses almost normally the SE part of the canal (Papanikolaou et al., 2015). It is a WSW-ENE trending, SSE dipping normal fault, with low slip rate (0.04 ± 0.02 mm/year according to Papanikolaou et al., 2015), but yet significant enough especially when important technical constructions can be influenced.

All of the sites studied in this paper are located at the foot wall of the above mentioned active fault, which was passively ruptured during the 1981 earthquake (which caused many damages at the canal walls) and according to a detailed leveling campaign (Mariolakos and Stiros, 1987) an overall displacement of 6cm was calculated, after the reinterpretation of the original geodetic data (Papanikolaou et al., 2015).
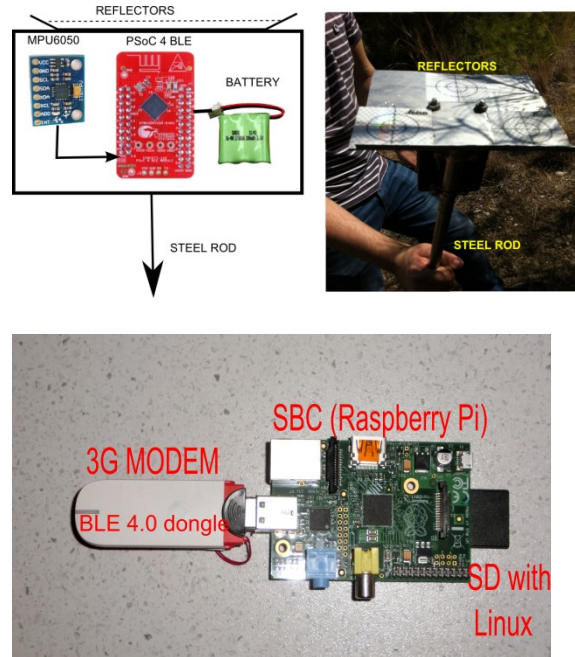
3 WSN Triggering Node

In the proposed study a set of WSN nodes is installed in the structure under investigation where they continuously monitor possible movement by operating as real time inclinometer. The Canal wall is treated as a 3D object which is expected to rotate at least in one of three orthogonal axes. For this purpose, each WSN monitors continuously possible rotations in (at least) one of the three orthogonal axes. Borrowing aviation terminology, the design of each WSN node continuously monitors Yaw, Pitch and Roll rotations. In the following, the description of the WSN node used for the monitoring network in this work is given.

3.1 Hardware Description

The hardware that is used in this work for building a WSN node comprises the PSoC 4 BLE (Bluetooth Low Energy) from Cypress Inc. (www.cypress.com). This PSoC is integrating a Bluetooth Smart radio, a high-performance 32-bit ARM® Cortex-M0 core with ultra-low-power modes, programmable analog blocks for sensor interfaces as well digital blocks for glue logic and control. The final outcome is a WSN node comprised only from a PSoC, a sensor MEMS and 3.6 battery cell.

The block diagram of the proposed WSN node is presented in Fig.2 (top). Inside the waterproof box there is a PSoC 4 BLE module, an Inertial Measurement Unit sensor (Invensense MPU-6050) and the cell battery. The MPU-6050 device combines a 3-axis gyroscope and a 3-axis accelerometer together with an onboard Digital

Motion Processor (DMP), which processes complex 6-axis algorithms. The whole construction was attached to a steel rod which is riveted to the examined structure

Fig. 2. (Top) Block diagram (left) and picture (right) of a WSN node. (Bottom)The coordinator module

The novelty of this project is the collaboration of the WSN node with terrestrial laser scanner measurements. Specifically, on the external side of the box an aluminum plate is attached in order to host three reflective targets for use with laser scanner. Data from the WSN node are sent to the coordinator module which operates as a Bluetooth to Internet router (through 3G network). The coordinator module (which is shown in Fig.2 (bottom)) consists of a commercial single board computer - SBC (Raspberry Pi), a BLE v4.0 dongle (for receiving Bluetooth data packets from WSN nodes) and a 3G modem (for connecting to Internet). SBC was preloaded with OpenWRT Linux distribution. Once the data from the WSN nodes are received, the router related processes pass them over 3G network to a remote server for post processing. Concurrently, a local process in SBC continuously checks if a predefined threshold reached and if so, an alert is issued to predefined users in order to begin a TLS procedure to the location of the corresponding WSN node. The power supply comes from solar cells which provide independence from

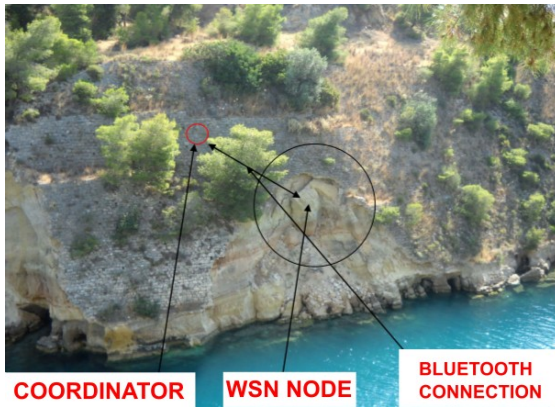power supply network. A typical installation presented in Fig.3

COORDINATOR **WSN NODE** **BLUETOOTH CONNECTION**

Fig. 3. Typical installation of single node. Red circle indicates the coordinator installation while black circle indicates the monitoring area

3.2 WSA Node Measurements

The purpose of WSN node is the continuous and real time measurement of Yaw, Pitch and Roll rotations (Fig.4) and the issue of an alarm signal in case, each (or all) of them exceed a predefined threshold.
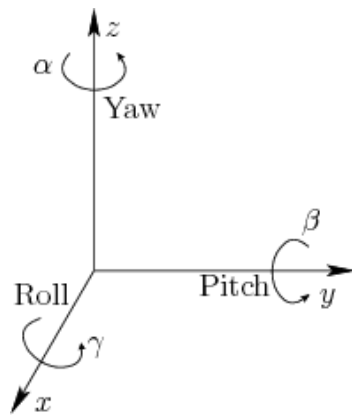

Fig. 4. A 3D rotation as a sequence of Yaw, Pitch and Roll rotations.

The calculation of the rotation angles can be made either by the accelerometer or the gyroscope. The use of IMU sensor in the WSN node, which combines an accelerometer and a gyroscope, increases the accuracy of the angle estimation while at the same time overcomes some limitations of each independent sensor. More specific, the accelerometer can provide the rotation (α, β and γ) angles but these values have a significant level of

uncertainty (mainly due to movement of the device). As a result, even if the accelerometer is in a relatively stable state, it is still very sensitive to vibration and mechanical noise in general. A solution that is proposed by the MEMS manufacturers is the concurrent use of gyroscope for smoothing out any accelerometer errors. However, the gyroscope still suffers from drift errors (Freescale, 2007; Microchip, 2012).

Both problems (acceleration data and gyroscope drift) can be solved using recursive filtering techniques. The well-known Kalman filter seems a reasonable choice but it was rejected because for this work the filtering process must take place in the WSN node and Kalman filter was quite hard to implement there. Instead of this, a complementary filter which acts as a long term – short term recursive adder and is very easy and light to implement making it perfect for embedded systems. On the long term, the data from the accelerometer are used because they do not drift. On the short term, the data from the gyroscope are used, because they are very precise and not susceptible to external forces. The complementary filter was implemented for each angle (α, β, γ). For one angle (i.e. the Yaw) the corresponding equation will be expressed as:

$$a = {}_{g} + {}_{\ldots} \cdot {}_{\ldots} + {}_{\ldots} \cdot {}_{\ldots} \qquad (1)$$

where:
c_g, c_a : filter tunable constants which must have sum 1 (in order to have a complementary filter that neither overshoots nor attenuates)
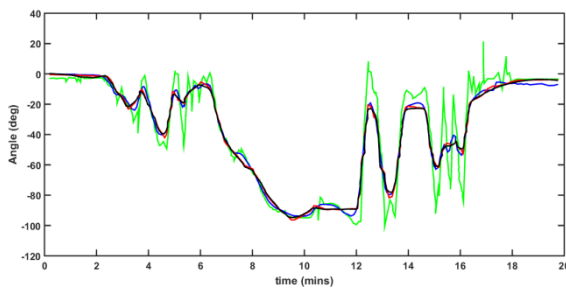G_{data} : gyroscope data
A_{data} : accelerometer data
dt : sampling rate

The gyroscope data are integrated every timestep with the current angle value. The integrated data are combined with the low-pass data from the accelerometer. After extensive trials it was concluded that c_g=0.97, c_a=0.03 and dt=8ms. At every iteration, the angle values are updated with the new gyroscope values by means of integration over time. The complementary filter then checks if the magnitude of the force measured by the accelerometer has an acceptable value that could be the real g-force vector. If the value is out of the predefined bounds, it is qualified as a disturbance and is not further taken into account. Consequently, the filter of Eq. (1) will update the angle with the accelerometer data by taking 97% of the current value, and adding 3% of the angle calculated by the

4

accelerometer. In this way it is ensured that the measurement will not drift (in the long term) while at the same time it will be very accurate on the short term.

Evaluation of the above approach is presented in Fig.5 where the measurements from the accelerometer, gyroscope and the output from the complementary filter are compared with the data from a high resolution inclinometer. Results are given for one axis only but the performance is similar for the other two axes. It is evident that the best results were derived by means of the complementary filter.

Fig. 5. Evaluation results from a laboratory controlled test.

In Fig. 5 the rotation angle was measured by a high resolution inclinometer (Jwell Instruments DXI 200) and shown in black solid line, the accelerometer are shown in green solid line and the gyroscope data in blue solid line. The output of the complementary filter (red solid line) follows quite successful the angle changes.
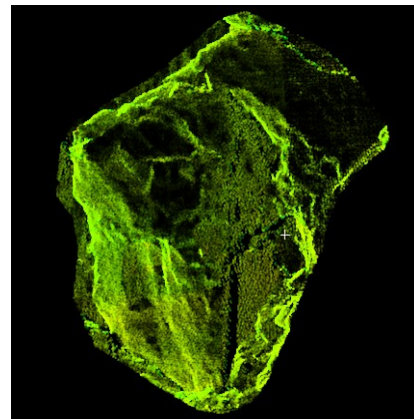
4 Experimental Data and Results

4.1 Data Collection

The data collection involved measurements from the WSN nodes and a terrestrial laser scanner (TLS). A number of WSN nodes were placed at selected points on the Canal walls. The node was collecting data continuously for three months, specifically from 27 July 2015 (start time 10:15:00hrs local) until 30 October 2015 (stop time 14:00:00hrs local). The sampling rate was set to 2Hz thus the number of collected samples were about 17.45×10^6.
The TLS used for the data collection was a Leica Scanstation 2. The data acquisition was performed in three different epochs for the slope depicted in Fig. 6. Specifically, data were collected on 10th June, 3rd July and 18th December of the year 2015.

In each measuring session, two scans were acquired at a resolution of 8x8mm. The chosen resolution was within the ideal point spacing of 86% of the beam width according to Lichti and Jamtsho (2006). The distance between the scanner and the object was less than 58m, which is well within the manufacturer's specifications. Fig. 6 shows an example of the registered point cloud for the scanned area indicated by the black circle (cf. Fig. 2). For the reference of the three different scans into the same coordinate system, direct georeferencing was used. In this way the scanner was set up over a known point (and its height over the point measured), was centred, levelled and oriented towards another known target where a spherical reflective target was set up (backsight), like a total station. The two points of the scanner and the target were known by total station surveying (uncertainty of few mm). The acquired scans taken from multiple scanner stations were already in the same reference system (Greek Geodetic Reference System of 1987, GGRS87) and then were easily compared with each other.

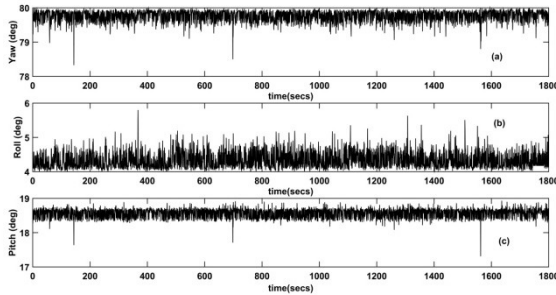**Fig. 6** Point cloud of the scanned wall area

4.2 Results

(a) WSN data

The characteristic patterns that were identified for the collected WSN data were three: a) quiet mode (which is the dominating one), b) ship-noise mode, and c) crack mode. For visualization purposes the three modes will be shown in separate graphs.
Fig.7 presents the collected data from the so called "quiet mode". This is the behavior that was record in the vast majority of the three-month
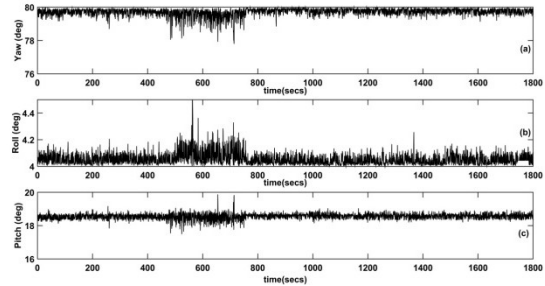
observation period. The interesting characteristic is the noise level of the WSN node which has: for Yaw, a mean value of 79.763 with standard deviation of 0.1646^o, for Roll, a mean value of 4.33^o with standard deviation of 0.2455^o and for Pitch, a mean value of 18.66^o with standard deviation of 0.1389^o. These values are consistent with the sensor's characteristics.
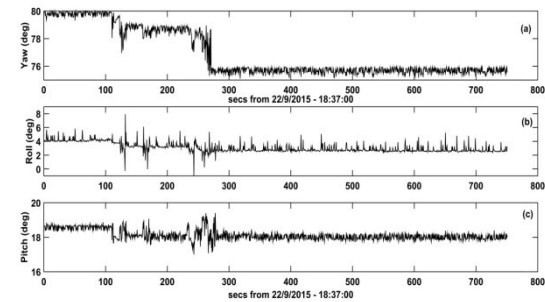

Fig. 7 Recording for quiet mode. (a) Yaw, (b), Roll and (c) Pitch rotations.

The second mode that was observed is the so called "boat-noise" which is frequent (at least twice per day) but not periodic. This is evidenced in Fig. 9 from 450sec to 800secs. It is expressed as a significant decrease in noise level which can affect the accuracy of the measurements. This phenomenon was observed when large ships pass the Corinth canal with size that is comparable to the width of the canal. A characteristic situation is presented in Fig. 8. Data that were contaminated by this type of noise were filtered before further processed.

The last mode that was observed was the "crack-mode" which fulfills the scope of the proposed device. The results are presented in Fig. 9 where the observed patterns can be described as follows: at t=110secs, a rotation begun which is more evident as Yaw rotation. This results at t=125secs to a new angle around 78° thus about -1.7^o from the previous stable position. Concurrently, a decrease of about 1° can be observed in the Pitch rotation. The Roll rotation presents a slight decrease of about 1°. These new values remain quite stable until 250secs. Then, an oscillation is observed in the Roll rotation which did not alter the previous values of the Pitch rotation. The interesting here is at the end of this oscillation (at around 280secs) a rapid decrease of about 2° was observed in the Yaw rotation. Stacking the previous results together, the final estimated of the rotations can be deduced as -4.4^o for Yaw, -1° for Roll and -1° for Pitch.
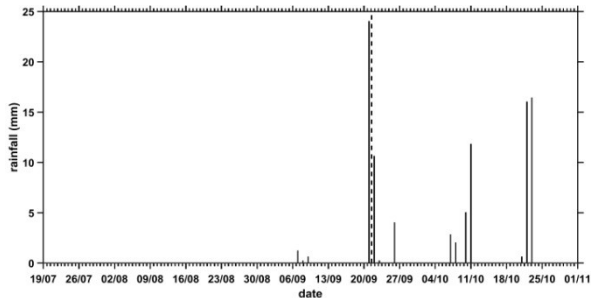

Fig. 8 Recordings for "ship-noise" mode. (a) Yaw, (b), Roll and (c) Pitch rotations. Noise level was increased at period from 450secs to 800 secs

Fig. 9 Recordings for "crack" mode. (a) Yaw, (b), Roll and (c) Pitch rotations. Significant changes can be observed in 100secs, 125secs and 250secs and 280secs (details in text)

The above findings are in good correlation with the weather conditions at the specific period. Specifically, using precipitation data (from the weather station network of the National Observatory of Athens (http://penteli.meteo.gr, last accessed on 15/11/2015) the graph of Fig. 10 is derived. It can be seen that the data marked with dashed line refer to the days with maximum precipitation during the whole observation period. These days coincide with the significant changes observed in Fig. 9.

Fig. 10. Precipitation data for the observing period (21/7/2015 – 30/10/2015). Time marker for results from Fig.4 marked with dashed line
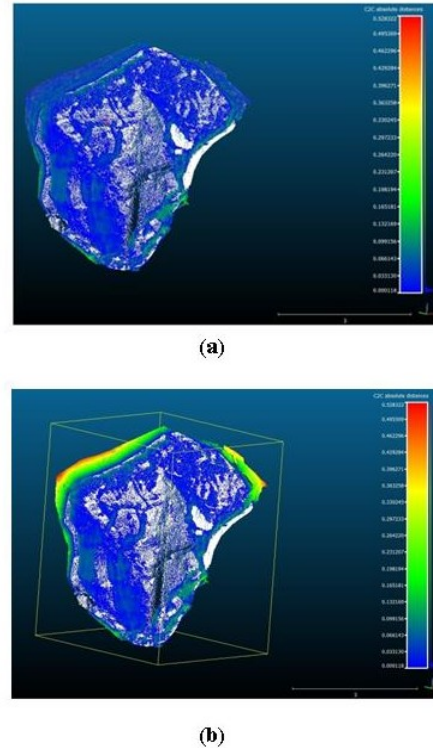
6

(b) TLS data

There are a number of different methods described in the literature with which scans from various epochs can be analyzed. The most common method is to compare GRID models generated from point clouds obtained before and after the deformation has occurred. Despite the fact that this method is simple to implement in commercial software, it offers limited sensitivity to small deviations in the positions of measuring points, and the measurement of changes in the object based on 3D point clouds can only be carried out in a single selected direction In this work a direct comparison of point clouds was performed since all scans were georeferenced at the same coordinate system, as discussed earlier.

The comparison of the registered scans acquired in each epoch was performed using the software CloudCompare. Fig. 11a shows the comparison between the first and second measuring epochs and Fig. 11b shows the comparison between the second and third epochs. The mean deviation in Fig. 11a is 0.014m ± 0.006m and in Fig. 11b is 0.084 m ± 0.009m.

The above results indicate that between the period from July to December 2015, a geometric change of the wall is depicted and coincides well with the results of the WSN node. The WSN data provided the information that an event has occurred. Then accurate geodetic techniques can augment the system with precise measurements.

Even though Landslides can have several causes, there is only one trigger that leads a near-immediate response in the form of a landslide. Observations and measurements have documented the triggers of landslides, which are commonly intense rainfall, earthquake shaking, volcanic eruption, storm waves, rapid stream erosion or human activities (Wieczorek, 1996)

Fig. 11. Comparison of point cloud data between measuring epochs

5 Concluding Remarks

The application of WSN which includes low-cost, but precise micro-sensors provides an inexpensive and easy way to set up a monitoring system in large areas. Using networks of inexpensive nodes as front end devices coupled with high resolution instruments that will be used only when the increased resolution is necessary, it can provide an efficient and safe way for the use of high-priced instruments.

This paper reported on the experience gained during the development of a project regarding a sensory system for monitoring the stability of a wall in the Corinth Canal. The focus of the project was the development of a WSN system specifically targeted for early warning purposes. More specific, the WSN nodes were used as triggering devices by continuous monitoring possible slope changes. In such case, an alert was produced and send to users in order to begin high resolution TLS. The preliminary results from a continuous four-month data collection showed that a change occurred in

late September with the values of the rotations being estimated as -4.4^o for Yaw, -1° for Roll and -1° for Pitch. The physical cause of rainfall resulted in the move of weak materials from the wall and showed with the above results.

The false alarm issue was present but its cause was recognized as it was due to the passes of large ships. The produced patterns in these cases could easily identified in data streams, leading to the characterization of these data as noise recordings and finally to reject them. The performance of the system during the data collection period was quite satisfactory since (after the rejection of aforementioned noise data) no false alarm was produced.

Coupling of the WSN warning system was performed with the use of terrestrial laser scanning that bridges the gap between point-wise monitoring with spatial coverage. The comparison between the georeferenced scan clouds acquired at three different epochs showed that a deviation of about 8cm was shown in the TLS data at the same time period as the results of the WSN data.

Even though the monitoring techniques have been improved significantly in the last years, the research in early warning systems for landslide monitoring is still under development and has quite a big room for improvement. It is clear that the application of such an early warning system demands multi-disciplinary knowledge. Future work will include the development of automatic startup devices coupled to TLS scanners in order to eliminate the need of human presence for their operation.

References

Anagnostopoulos, A.G., N. Kalteziotis, G.K. Tsiambaos, M. Kavvadas (1991). Geotechnical properties of the Corinth Canal marls. *Geotech Geol Eng*, 9(1), 1-26.

Anastasi, G., G. Lo Re, M. Ortolani (2009) WSNs for structural health monitoring of historical buildings. In: *Proc. Human System Interactions, HSI '09*, 21-23 May, Ctania, Italy.

Buratti, C., A. Conti, D. Dardari, R. Verdone (2009) An Overview on Wireless Sensor Networks Technology and Evolution. *Sensors*, 9(9), 6869-6896; doi:10.3390/s90906869.

Chang, D.T.T. Y. Chung, LL Guo, K. Chun, C. Yang, Y-S. Tsai (2011) Study of Wireless Sensor Network(WSN) using for slope stability monitoring. In: *Proc. Int. Conference on Electric Technology and Civil Engineering (ICETCE)*, IEEE, 22-24 April, Lushan, pp 6877-6880.

Collier, R.E.L., J. Thompson (1991). Transverse and linear dunes in an Upper Pleistocene marine sequence, Corinth Basin, Greece. *Sedimentology*, 38(6), 1021-1040.

Collier, R.E.L., M.R. Leeder, P.J. Rowe, T.C Atkinson (1992). Rates of tectonic uplift in the Corinth and Megara Basins, central Greece. *Tectonics*, 11(6), 1159-1167.

Culler, D., D. Estrin, M. Srivastava (2004). Overview of sensor networks. *IEEE Comput. Mag.* 2004, *37*, 41–49.

Freescale Semiconductors (2007), Implementing Auto-Zero Calibration Technique for Accelerometers. App. Note 3447

Gkika, F., G-A. Tselentis, L. Danciu *(2005)*. Seismic risk assessment *of* Corinth Canal. Greece. *Coastal Engineering VII,* WIT Press, Southampton, pp.323-332.

Lichti, D. and Jamtsho, S.: Angular resolution of terrestrial laser scanners, Photogrammetric Record, 21(114), 141–160, 2006.

Marinos, P., G. Tsiambaos, (2008). The geotechnics of Corinth Canal: a review. *Bulletin of the Geological Society of Greece* XXXXI/I, 7-15.

Mariolakos, I., S.C. Stiros, (1987). Quaternary deformation of the Isthmus and Gulf of Corinthos (Greece). *Geology*, 15(3), 225-228.

MicrochipTechnology (2012), Implementing Motion Sensing Capabilities on PIC24 Microcontrollers, App.Note 1440,

Papanikolaou, I.D., M. Triantaphyllou, A. Pallikarakis, G. Migiros (2015). Active faulting at the Corinth Canal based on surface observations, borehole data and paleoenvironmental interpretations. Passive rupture during the 1981 earthquake sequence? *Geomorphology*, 237, 65-78.

Paek, J., N. Kothari, , K.Chintalapudi, S. Rangwala, N. Xu, J. Caffrey, R.Govindan, S. Masri, J. Wallace, D. Whang (2005).The Performance of a Wireless Sensor Network for Structural Health Monitoring. In: Proc. 2nd *IEEE Workshop on Embedded Networked Sensors* (EmNetS-II), 30-31 May.

Wieczorek, G. F.(1996). Landslide Triggering Mechanisms. In A. K. Turner & L. R. Schuster (Eds.), Transportation Research Board Special Report 247: *Landslides: Investigation and Mitigation* (pp. 76-90). Washington D. C.